

Key issues in the characterization of porous PZT based ceramics with morphotropic phase boundary composition

L. Pardo · A. García · K. Brebøl · D. Piazza · C. Galassi

Received: 13 March 2006 / Accepted: 4 August 2006 / Published online: 28 February 2007
© Springer Science + Business Media, LLC 2007

Abstract An iterative automatic method is used to calculate, from impedance measurements at resonance in three sample shapes and four modes of resonance, all the directly obtained coefficients that are needed to determine the ten elastic, dielectric and piezoelectric complex coefficients of the characteristic matrix of a 6 mm symmetry ferro-piezoelectric ceramic for a controlled porosity material. A soft PZT ceramic with a Morphotropic Phase Boundary (MPB) composition was studied. Samples with homogeneously distributed close porosity were prepared and tested. A fugitive phase was added to the perovskite type structure precursor powder to produce the porous materials and the samples were consolidated by die pressing. Shear coefficients are here obtained using an alternative geometry to the Standards shear sample, that was proved to be dynamically clamped at resonance. Comparison of these shear results and those obtained with the geometry of the Standards is here discussed and the advantages for the shear characterization of porous ceramics derived from the use of this new geometry are presented.

Keywords Piezoelectricity · Porous PZT · Losses · Shear resonance mode · Standards

L. Pardo (✉) · A. García
Instituto de Ciencia de Materiales de Madrid,
Consejo Superior de Investigaciones Científicas (ICMM-CSIC),
Cantoblanco, 28049 Madrid, Spain
e-mail: lpardo@icmm.csic.es

K. Brebøl
Limiel ApS, Langebæk, Denmark

D. Piazza · C. Galassi
National Research Council Institute of Science and Technology
for Ceramics (ISTEC-CNR),
via Granarolo 64, 48018 Faenza, Italy

1 Introduction

Characterization of piezoceramics in the linear range from impedance data at resonance is a widespread practice and standard methods of measurements have been issued long time ago and revised several times [1–3]. The three material resonator shapes (Fig. 1) and four modes of resonance shown in Table 1 are sufficient for the purpose of the full matrix characterization, including all losses, of piezoceramics [1] from impedance measurements at resonance. Table 1 also shows the directly obtained coefficients for each mode. The systematic application of Alemany et al. automatic iterative method to the full matrix characterization of a Navy II Type PZT commercial piezoceramic [4], PZ27 from Ferroperm Piezoceramics A/S, using the three sample shapes and four resonance modes of Table 1, has been recently published. The accuracy of the results of the modeling of piezoelectric devices by numerical methods, as the Finite Element Analysis (FEA), relies on the accuracy of the material parameters used and thus matrix characterization of piezoceramics is a key issue for the development of new devices.

Iterative or fitting methods have been used also by other authors in the full matrix characterization of piezoelectric composites [7] and partial characterization of composites and polymers [8], as well as porous piezoceramics [9], showing advantages with respect to the 1987 IEEE Standard procedures [2] in the characterization of lossy materials.

It is well-known that the porous piezoceramics have enhanced properties with respect to dense ceramics for applications like some types of low frequency hydrophones and sensors, due to their better hydrostatic figures of merit (d_{hg}) [10–12]. However, the porous ceramics characteristics, namely, the low mechanical quality factors and electromechanical coupling coefficients, limit the applica-

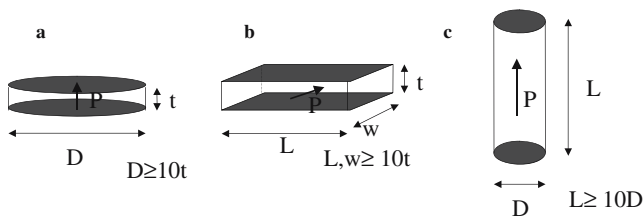


Fig. 1 The three piezoceramic standard sample shapes needed for the determination of the full matrix of coefficients for a 6 mm symmetry piezoelectric material: **a** thin disks, thickness poled, **b** shear plates and **c** long bars, length poled. P=sample polarization

tion of the 1987 IEEE [2] and CENELEC [3] Standard measurement methods in their characterization.

Porous ceramics present additional difficulties in their full matrix characterization, which requires the use of all the three sample shapes of Fig. 1. It has been proved that nonlinearities (S-E and P-E cycles) are similar in dense ceramics and in porous ceramics with up to 45% porosity [13], well below the percolation threshold in bulk (85%). However, surface inhomogeneity, or defects introduced while cutting or grinding the sample, easier in porous than in dense ceramics, may cause that some of the required sample shapes, namely the shear plates and the length poled long bars (Fig. 1), were specially difficult to pole when working with porous piezoceramics. Also, the breakdown fields of polycrystals are reduced as the total porosity and pore size [14] increases, making difficult the application of the high fields needed during the poling of such sample shapes.

Besides, recent work of some of the authors [15] has shown that the use of the Standard shear sample (Fig. 1), leads to underestimation of the shear coefficients which, according to results of the modeling of the resonances of this sample by FEA, is due to a dynamical clamping of the sample. An alternative material shear resonator has also been suggested [16].

To overcome some of the difficulties arising in the linear characterization of porous piezoceramics, this work presents a discussion on the application of Alemany et al. automatic iterative method [5, 6] to three sample shapes and four modes of resonance needed for a 6 mm symmetry material matrix characterization from complex impedance measurements. The complex shear coefficients are here measured on a non-standard shear geometry and comparison is given with the results of a Standards sample.

Table 1 The three sample shapes and four modes of resonance needed for the full characterization of ferro-piezoelectric ceramics with 6 mm symmetry.

Sample geometry	Resonance mode	Directly obtained coefficients
Thin disks, thickness poled	Thickness extensional mode of thin plates	$h_{33}, e_{33}^S, c_{33}^D$
	Radial mode of thin disks	$d_{31}, e_{33}^T, s_{11}^E, s_{12}^E$
Shear plates	Thickness shear mode of thin plates	$h_{15}, e_{11}^S, c_{55}^D$
Long bars, length poled	Length extensional mode of long bars	$g_{33}, e_{33}^T, s_{33}^D$

2 Experimental procedures

2.1 Sample processing and characterization

Porous ceramic samples of the composition $Pb_{0.988}(Zr_{0.52}, Ti_{0.48})_{0.976}Nb_{0.024}O_3$ were used in this study. The starting oxides were: PbO (Aldrich 99.9%), ZrO_2 (MEL SC101 of 99.7%), TiO_2 (Degussa P25, 99.5%) and Nb_2O_5 (Aldrich 99.9%). Dense samples were prepared for comparison by directly die pressing the precursor powder obtained by the solid state reaction of the starting oxides at 850 °C for 4 h [17]. The porous samples were obtained by adding 50 vol.% of carbon black as pore former to the same perovskitic powder. The homogenization by ball milling was followed by the die pressing of the dry powders and sintering. Sintering conditions and final density are reported in Table 2. The evaporation of the carbon powder added to the PZT powder was investigated by DTA (differential thermal analysis) and TG (thermogravimetric analysis) as well as by carefully controlling the weight loss during sintering of the PZT powder added with graphite. Furthermore, the DC resistivity and AC dielectric spectroscopy (100–100 kHz) shows the absence of percolative paths of carbon deposit. The SEM image of a polished surface of the porous sample is shown in Fig. 2, revealing that porosity mainly consists on close pores.

2.2 Piezoelectric characterization

The samples were ground to remove surface layers, screen printed with silver electrodes, fired at 700 °C and finally poled in silicon oil at 120 °C, under a dc field of 3 kV/mm for 40 min. The total porosity (about 39% in the porous samples) was calculated from the final density, average $4,89 \text{ g}\cdot\text{cm}^{-3}$, calculated as the ratio between the weight of the dry sample and the volume obtained from the sample dimensions.

The following ceramic resonator shapes and dimensions (Fig. 1) were studied in this work: (1) thin disks, thickness poled, of $t=1,00$ mm thickness and $D=21,50$ mm diameter, used to determine parameters from the radial and thickness resonance modes, (2) length poled long bars of $L=10,07$ mm length, and $2,01 \times 2,01 \text{ mm}^2$ square section, (3) non-standard thickness shear plates, thickness poled, of $t=10,04$ mm length between electrodes for measuring, $L=1,21$ mm poled

Table 2 Sintering conditions and density of the studied samples.

Sample	Sintering temp °C	Density g/cm ³	Density %
Dense PZTN	1,200–2 h	7.81–7.85	97.5–98.0
Dense PZTN	1,150–1 h	7.63	95.3
Porous PZTN (carbon black 50 vol.%)	1,150–1 h	4.85–4.93	60.6–61.6

thickness and $i=10,00$ mm width and, finally, and for the sake of comparison, (4) standard thickness shear plate resonators, length poled, of $t=1,25$ mm of thickness between electrodes for measuring, $L=10,47$ mm poled length and $w=9,99$ mm width.

Currently more than one sample of each type was measured and the results showed here are representative of the material behaviour.

The automatic iterative method to determine shear coefficients from impedance measurements for the non-standard thickness shear plate is similar to the ones used for the Standards thickness plate or shear plate, that were described elsewhere [5].

Only the dimensions and density of the sample, together with the value of the complex admittance or impedance at four frequencies around the resonance, chosen automatically in each iteration step to solve the analytical expression of the immittance, obtained from the wave equation of a given resonance mode, are required to get the coefficients associated with a resonance mode (Table 1). The full spectra is nevertheless measured and after finishing the calculation, as a quality criteria of the results obtained by the method, both the G and the R profiles are reconstructed by insertion of the calculated complex coefficients into the analytical solution of the wave equation of the given resonance mode (to calculate of R and G as a function of the frequency). When the experimental resonance spectra is

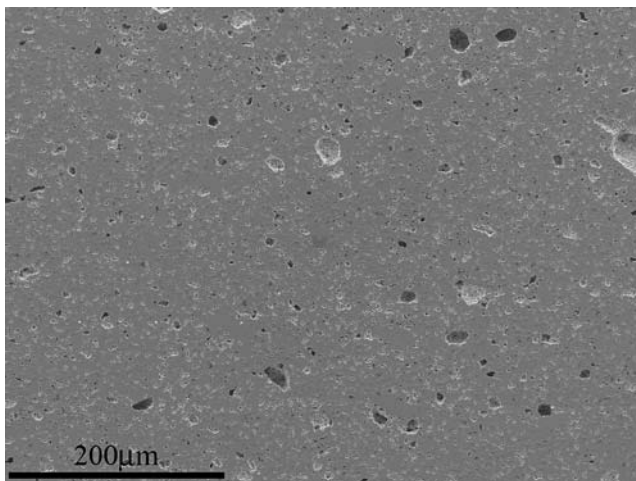


Fig. 2 SEM image of a polished surface of the porous sample

free of spurious resonances, thus corresponding to a single resonator, the regression factor between the experimental and reconstructed values is normally higher than 0.99.

3 Experimental results

Figure 3 and Table 3 shows the measured and recalculated spectra and results of the characterization at the thickness and radial modes of the thin disk, thickness poled. Figure 4 and Table 3 shows the results of the characterization of the thickness extensional mode of the long bar, length poled.

The good agreement between the experimental data and the reconstructed by the use of the parameters obtained by Alemany et al. method is clear for the resonances mentioned, that indicates the accuracy of such values. Despite of the fact that they are not a clean unique resonance, the thickness vibration of the thin disks and the long bar have regression factors for such reconstruction of 0.967 and 0.912, respectively (Figs. 3a and 4), whereas

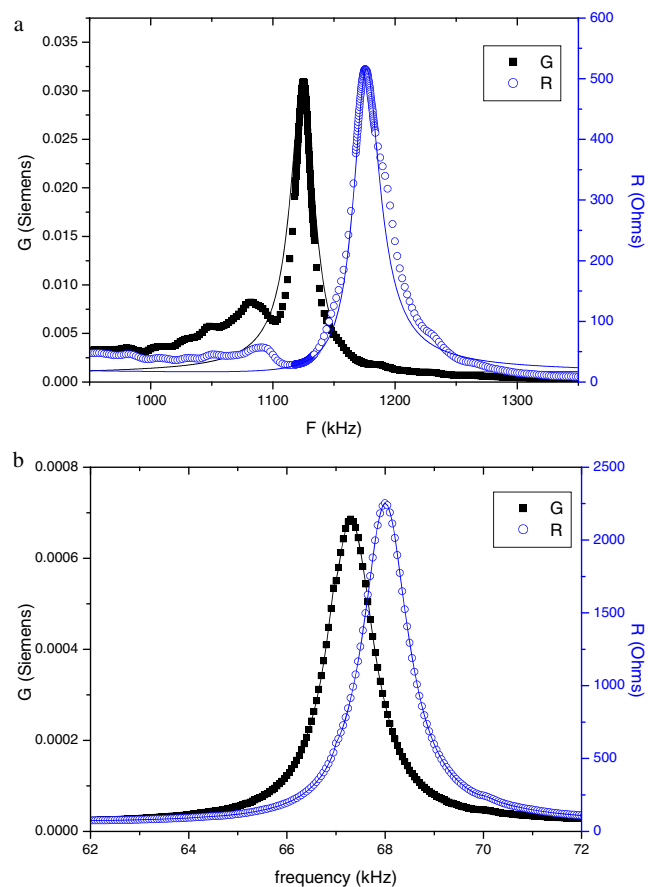


Fig. 3 Conductance, G , and resistance, R , profiles for a porous ceramic sample and for: **a** the fundamental thickness shear resonance mode of a thin disk, thickness poled, and **b** the fundamental radial resonance mode of a thin disk. Reconstructed values after Alemany et al. method calculated values are shown. (Symbols=experimental G and R values, lines = reconstructed G and R values)

Table 3 Coefficients obtained for each mode of resonance of the thin disk and long bar.

Type of resonance	Material parameters	Type of resonance	Material parameters	Type of resonance	Material parameters
Thickness mode of thin disk		Planar mode of thin disk		Length mode of long bar	
$ K_t $ (%)	31.9	$ K_{pl} $ (%)	15.5	$ K_{33} $ (%)	36.3
N_t (kHz.mm)	1,125	$ K_{31} $ (%)	9.3	N^l (kHz.mm)	1,170
		N_p (kHz.mm)	1,423		
		Coeff. Poisson (σ^p)	0.282		
c_{33}^D ($10^{10} N.m^{-2}$)	2.70+0.06 i	s_{11}^E ($10^{-12} m^2.N^{-1}$)	45.15-0.77 i	s_{33}^D ($10^{-12} m^2.N^{-1}$)	33.24-0.66 i
c_{33}^E ($10^{10} N.m^{-2}$)	2.43+0.05 i	s_{12}^E ($10^{-12} m^2.N^{-1}$)	-12.82+0.22 i	s_{33}^E ($10^{-12} m^2.N^{-1}$)	38.27-0.68 i
		s_{66}^E ($10^{-12} m^2.N^{-1}$)	115.94-1.99 i		
		s_{11}^D ($10^{-12} m^2.N^{-1}$)	45.69-0.74 i		
h_{33} ($10^{-12} C.N^{-1}$)	10.06+0.87 i	s_{12}^D ($10^{-12} m^2.N^{-1}$)	-13.38+0.21 i	d_{33} ($10^{-12} C.N^{-1}$)	166.35-5.65 i
		d_{31} ($10^{-12} C.N^{-1}$)	-39.32+0.62 i	g_{33} ($10^{-3} m.V.N^{-1}$)	30.21+0.9 i
ϵ_{33}^S	302-42 i	ϵ_{33}^T	416-13 i	ϵ_{33}^T	621-40 i

Marked in bold those coefficients directly obtained by solving the equation of movement in each mode, to be used for the matrix characterization.

for the radial vibration of the thin disk, almost unperturbed, the regression factor raises up to 0.996.

Figure 5 shows the spectra of resonance of the two shear plates. The standard shear sample presents double peaks, Fig. 5a. Under this circumstances is feasible, in this particular case, but always meaningless, a blind calculation by Alemany et al. method, which is based on the assumption that the measured values corresponds to a single resonator performance. The results of this blind calculation are nevertheless shown in Table 4, and the unacceptable reconstruction of the spectra resulting from the obtained values is also shown in Fig. 5a. The non-standard shear sample shows a less perturbed spectra, nevertheless with some satellite resonances, and the results of the calculation of the corresponding coefficients are also shown in Table 4.

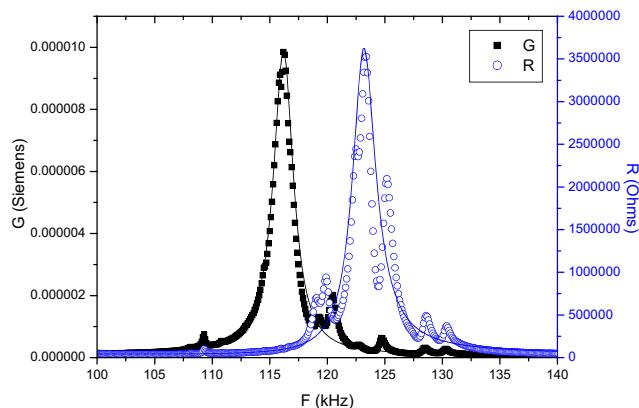


Fig. 4 Conductance, G , and resistance, R , profiles for a porous ceramic sample and for the fundamental thickness extensional mode of a length poled long bar. Reconstructed values after Alemany et al. method calculated values are shown. (Symbols=experimental G and R values, lines = reconstructed G and R values)

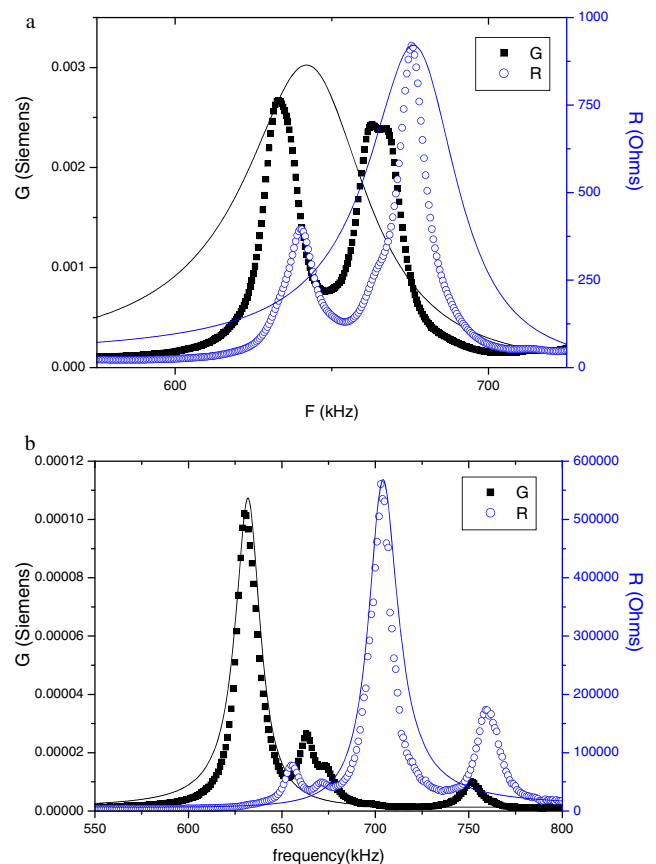


Fig. 5 Conductance, G , and resistance, R , profiles for porous ceramic samples and for: **a** the fundamental thickness shear resonance mode spectra of a Standard shear sample, and **b** the fundamental thickness shear resonance mode of the alternative shear sample here presented. Reconstructed values after Alemany et al. method calculated values are shown. (Symbols=experimental G and R values, lines = reconstructed G and R values)

Table 4 Coefficients obtained for the fundamental shear resonance modes of the standard and the non-standard shear samples used here.

Type of resonance and parameters	Shear mode of a standard plate	Shear mode of a non-standard plate
k_{15} (%)	34.44	48.9
N_{15} (kHz.mm)	791	7962
$c_{55}^D (10^{10} N.m^{-2})$	1.40+0.07 i	1.50+0.04 i
$c_{55}^E (10^{10} N.m^{-2})$	1.24+0.10 i	1.14+0.03 i
$s_{55}^D (10^{-12} m^2.N^{-1})$	71.11–3.61 i	66.47–1.84 i
$s_{55}^E (10^{-12} m^2.N^{-1})$	80.29–6.25 i	87.35–2.22 i
$h_{15} (10^8 V.m^{-1})$	5.33–0.36 i	12.69+0.86 i
$e_{15} (C.m^{-2})$	3.11–0.26 i	2.82–0.09 i
$d_{15}^{15} (10^{-12} C.N^{-1})$	247.76–40.66 i	246.47–14.30 i
ϵ_{11}^S	744–34 i	328–32 i
ϵ_{11}^E	658–12 i	250–25 i

Marked in bold those coefficients directly obtained by solving the equation of movement for each shear mode, to be used for the matrix characterization.

4 Discussion

Difficulties in getting a coherent set of data from different sample shapes and resonances arise on the dispersive character of the piezoceramics and the dependence of their properties on the polarization level, which may became a key issue in the matrix characterization of porous ceramics.

Due to the dispersive character of the dielectric constant in piezoceramics, there is always a difference between the dielectric permittivity, ϵ_{33}^T , of the thin disk and the long bar, measured here at the resonances in the 64–70 kHz ($\epsilon_{33}^T = 416 - 13 i$) and 110–130 kHz ($\epsilon_{33}^T = 621 - 40 i$), intervals respectively. The expected variation should be a decrease of permittivity as the frequency increases, whereas Table 3 shows the contrary trend. This result can be understood as due to the different polarization level achieved in both sample shapes, the long bar having a lower level. These results then show that the polarization of the long bar is thus a key issue, that must be solved for the matrix characterization. In any case, due to the dispersion of the material, the ϵ_{33}^T considered for the calculations involved in the matrix characterization is the average of the two measured values for the thin disk and the long rod [4].

The presence of two peaks of similar intensity at the resonance spectra of the Standard shear sample has been observed previously, and can also be ascribed to inhomogeneous polarization corresponding to a low polarization level achieved [18]. This fact, coupled to the dynamical clamping of the Standard [15], severely limits the application of the solution obtained by the Alemany et al. method in the matrix characterization. As an example, data in Table 4 show that all elastic losses, as revealed by the imaginary part of the elastic coefficients, determined from

the Standard sample are much higher than those determined for the non-standard one. Besides, here also the dielectric permittivity show to be very sensitive to the polarization level, being much higher for the insufficiently poled Standard shear element (Table 4). Alemany method can, in some instances, be used to obtain reliable values for two clearly separated resonances [17], corresponding to two polarization levels in the sample, but this is not the case here, as Fig. 5a shows. Double resonances of that type are also impossible to be used for any of the methods developed by other authors based on experimental curve fitting [8].

The poling of the non-standard geometry here studied, as an alternative geometry to the Standard shear, has similar difficulties, but not additional, to the poling of thin porous piezoceramic disks. As a result, the main shear resonance of the non-standard sample can be solved with reasonable accuracy by Alemany et al. method. The regression factor of the reconstructed to the experimental data, despite of the fact that the spectra does not present a single resonance, is 0.830, as compared with 0.008 in the Standard element. The electromechanical coupling coefficient obtained in the non-standard shear sample is 42% higher that the one evaluated from the Standard sample.

With all the data here obtained by the Alemany et al. method and with the use of an alternative geometry to the Standard shear sample, the calculation of the full complex matrix of elastic, piezoelectric and dielectric coefficients can be carried out as explained elsewhere [4]. Finally, as a necessary consistency criteria among the coefficients of the matrix obtained [16], in particular concerning the measured or calculated losses, the Holland criteria [19] should be applied and fulfilled for the material to ensure a passive material not generating energy.

5 Conclusions

The study of all the sample shapes and resonance modes needed for the full matrix characterization, including losses, of a porous PZT based piezoceramic with MPB composition has been carried out by Alemany et al. automatic iterative method, from immittance measurements at resonance.

It was observed that the use of a Standard shear sample for matrix characterization of a porous ceramic is not possible due to the low polarization level achievable, that adds to the effect of the dynamical clamping of such sample. A non-standard shear geometry is here recommended as a realizable alternative for porous ceramic characterization. Besides, this non-standard shear sample allows characterization from identically poled samples at the thickness, radial and shear modes of resonance.

Acknowledgements This work has benefited from the synergy provided by the POLar ELEctroCERamics, POLECER, (G5RT-CT2001-05024) Thematic Network of the EC GROWTH Program under the Fifth RTD Framework Program. Mr. A. García acknowledges the POLECER linked grant at ICMM-CSIC. Mr. D. Piazza acknowledges the POLECER Short Term Scientific Mission at ICMM. Authors are also indebted to Dr. C. Alemany (ICMM-CSIC, at the time of writing this paper already retired) for the generous implementation of the automatic iterative method to the second thickness shear geometry here used.

References

1. Proc. IRE, **49**(7), 1161–1169 (1961)
2. ANSI/IEEE Std. 176–1987
3. European Standard CENELEC, EN 50324-2
4. M. Alguero, C. Alemany, L. Pardo, A.M. Gonzalez, J. Am. Ceram. Soc. **87**(2), 209 (2004)
5. C. Alemany, L. Pardo, B. Jimenez, F. Carmona, J. Mendiola, A. M. González, J. Phys. D: Appl. Phys. **27**, 148 (1994)
6. C. Alemany, A.M. Gonzalez, L. Pardo, B. Jiménez, F. Carmona, J. Mendiola, J. Phys. D: Appl. Phys. **28**(5), 945 (1995)
7. Sherrit, H.D. Wiederick, B.K. Mukherjee, Smart Materials, Structures, and Integrated Systems. SPIE Proc. **3241**, 327 (1997)
8. K.W. Kwok, H.L.W. Chan, C.L. Choy, IEEE Trans. Ultrason. Ferroelectr. Freq. Control **44**(4), 733 (1997)
9. G. Fabbri, C. Galassi, F. Cracium. Ferroelectrics **293**, 291–305 (2003)
10. K. Brebøl, L. Pedersen, W.W. Wolny, Proc. of 1990 IEEE 7th Int. Symp. on Applications of Ferroelectrics, June 6–8, 1990, Illinois, USA. IEEE Cat.no. 90CH2800-1. pp. 18–21
11. S. Marselli, V. Pavia, C. Galassi, E. Roncari, F. Cracium, G. Guidarelli, J. Acoust. Soc. Am. **106**, 733 (1999)
12. A. Perry, C.R. Bowen, H. Kara, S. Mahon, Key Eng. Mater. **206–213**, 1505 (2002)
13. F. Cracium, C. Galassi, E. Roncari, Europhys. Lett. **41**, 55 (1998)
14. R. Gerson, T.C. Marshall, J. Appl. Phys. **30**(11), 1650–1653 (1959)
15. L. Pardo, M. Alguero, K. Brebøl, J. Phys. IV (France) **128**, 207–211 (2005)
16. L. Pardo, M. Alguero, K. Brebøl, J. Phys. D: Appl. Phys. (in press)
17. C. Galassi, E. Roncari, C. Capiani, A. Costa, *NATO Science Series 3—High Technology*, vol. 76, eds. By C. Galassi, M. Dinescu, K. Ukino, M. Sayer (Kluwer, Massachusetts, 2000), pp. 75–86
18. M. Alguero, C. Alemany, L. Pardo, M.P. Thi, J. Am. Ceram. Soc. **88**(10), 2780–2787 (2005)
19. R. Holland, IEEE Trans. Sonics Ultrason. **SU-14**(1), 18 (1967)